THE JOURNAL OF PHYSICAL CHEMISTRY B LETTERS

2005, *109,* 15687−15690
Published on Web 08/04/2005

Polarized Surface-Enhanced Raman Spectroscopy on Coupled Metallic Nanowires

Andrea R. Tao[†] and Peidong Yang*[,†,‡]

Department of Chemistry, University of California, Berkeley, California 94720, and Materials Science Division, Lawrence Berkeley National Laboratory, Berkeley, California 94720

Received: June 21, 2005; In Final Form: July 15, 2005

Regular-shaped metal nanocrystals and their ensembles can serve as ideal substrates for studying surface-enhanced Raman scattering (SERS). We synthesized well-defined silver nanowires for a systematic study of SERS signal with respect to polarization and structural ordering. The observed dependence on polarization direction confirms prior theoretical predictions that large electromagnetic (EM) fields are localized in the interstitials between adjacent nanowires. We show that these modes are largely dipolar in nature and rely on short-range EM coupling between nanowires.

Surface-enhanced Raman spectroscopy (SERS) is a powerful tool for chemical analysis with its molecular specificity and extraordinary sensitivity capable of single-molecule detection. For molecules adsorbed to nanostructured metal surfaces, Raman cross sections have been reported to increase by 10^{12}.[1,2] In addition to gaining fundamental insight on this enhancement phenomenon, a range of interesting applications have been proposed, from noninvasive biological detection to single-nucleotide identification in DNA sequencing.[3]

Many theoretical SERS studies have placed emphasis on electromagnetic (EM) field enhancement, in addition to any chemical enhancement mechanism. When light is absorbed by a rough metal surface, it will excite the collective oscillations of conduction electrons, known as a surface plasmon. This plasmon excitation, which coherently couples to an external field, produces local field amplification. According to classical EM theory, surface enhancement scales as the fourth power of the total electric field according to

$$I_{\mathrm{SERS}} \propto \left|\frac{E(\omega)}{E_0(\omega)}\right|^2 \left|\frac{E(\omega_s)}{Eo(\omega_s)}\right|^2 \qquad (1)$$

where $E(\omega)$ and $E(\omega_s)$ are the enhanced local fields at the excitation and scattering frequencies, respectively, and E_0 is the incident field. Recently, computational models have predicted that large EM fields localized in the junction between metal structures can be generated upon irradiation with light.[4−6] These local fields are believed to be the Raman "hot spots" that dominate the observed SERS signal for rough metal surfaces.[7] The majority of recent SERS work has been conducted on silver or gold thin films,[8−13] lithographically fabricated surfaces,[14−16] or nanoparticle aggregates,[4,17,18] most of which are geometrically ill-defined at the nanoscale. Recently, we and others have examined the rational design of high-response SERS substrates by assembling 2-D arrays of metal nanoparticles and nanowires by Langmuir−Blodgett deposition.[19−22]

Here, we perform a detailed and systematic examination of these nanowire arrays in order to gain a better understanding of the EM modes responsible for surface enhancement. We fabricated aligned films of silver nanowires and measured Raman intensities of chemisorbed 1-hexadecanethiol. The observed dependence on polarization direction confirms prior theoretical predictions that large EM fields are localized in the interstitials between adjacent nanowires. We show that these modes are largely dipolar in nature and rely on short-range EM coupling between nanowires.

Compared to past SERS experiments, this study relies on the use of metal surfaces that are well defined at both the microscale and nanoscale. We synthesized silver nanowires using the polyol method with poly(vinyl pyrolidone) (PVP) as a surface-capping agent to promote one growth direction.[19] PVP is thought to stabilize the (100) faces of the nanowire by selective adsorption, permitting further metal reduction only at the relatively unprotected (111) surface.[23] Scanning electron microscopy (SEM) images show the wires are 45 ± 5 nm in diameter and 1.57 ± 0.07 μm long (Figure 1a, inset). The wires possess pentagonal cross sections and sharp vertices. Transmission electron microscopy (TEM) confirmed that the nanostructures are composed of five single-crystalline domains with atomically smooth surfaces. These well-defined surfaces allow for an unambiguous description of the molecular orientation and environment of adsorbate species.

The as-prepared wires were incubated with 1-hexadecanethiol, which served as the probe molecule for our Raman studies. Hexadecanethiol readily forms a well-ordered monolayer on silver surfaces and does not experience any resonance Raman effects.[24] The wires were aligned into densely packed monolayers and deposited onto copper TEM grids (at a surface pressure of $\pi = 24$ mN/m^2) using the Langmuir−Blodgett technique.[19] A typical SEM image of a well-aligned monolayer is shown in Figure 1a. Nanowire density is on the order of 10^{12} nanowires/m^2. Samples were kept under vacuum ($\sim 10^{-2}$ Torr) until Raman experiments were carried out.

We used a Renishaw micro-Raman system equipped with a half-wave plate and polarizer for all SERS experiments. The experimental geometry is arranged for 180° backscattering, as

* To whom correspondence should be addressed. E-mail: p_yang@berkeley.edu
[†] University of California, Berkeley.
[‡] Lawrence Berkeley National Laboratory.

10.1021/jp053353z CCC: $30.25

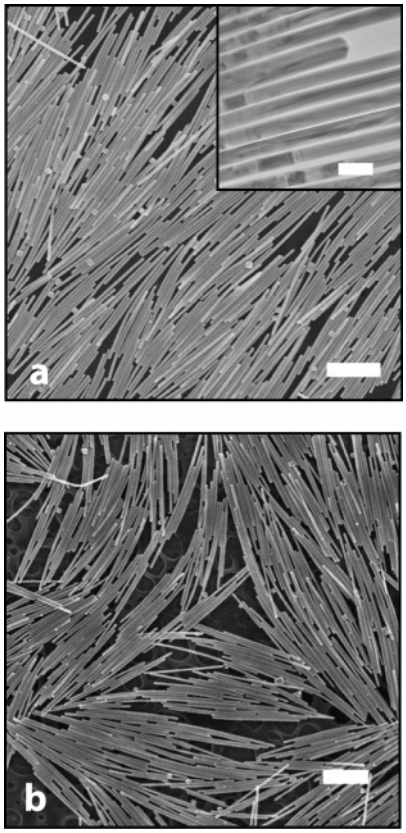

Figure 1. SEM images of silver nanowire monolayers with varying degrees of order. The order parameter, *S*, characterizes the overall orientation alignment of the sample, with perfect alignment for $S = 1$: (a) $S = 0.970$; (b) $S = 0.354$. Scale bar = 1 μm. The inset shows a TEM image of the nanowires, with pentagonal cross sections and an atomically smooth surface. Scale bar = 50 nm.

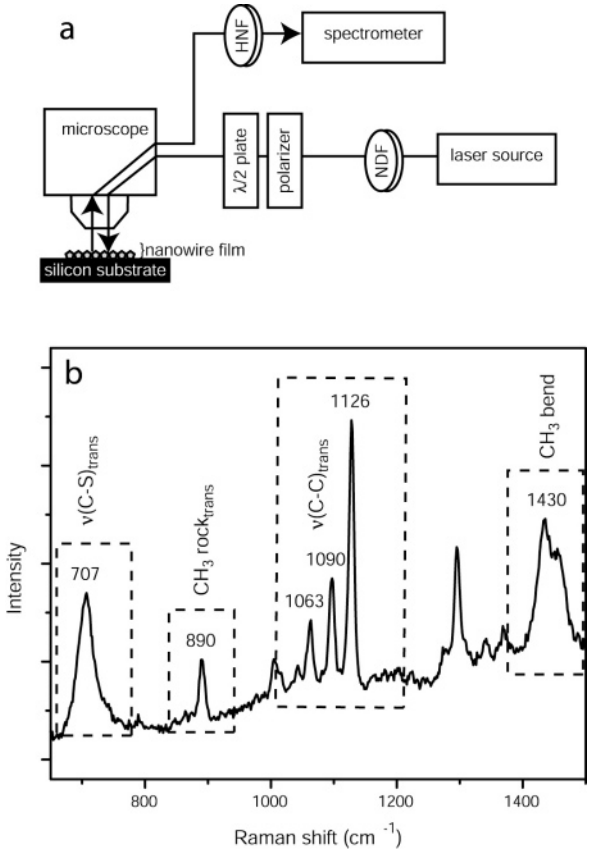

Figure 2. (a) Schematic illustration showing the micro-Raman experimental setup used for the 180° backscattered SERS experiments. A 532 nm solid-state laser is used as the irradiation source. Polarization of incident light is controlled by rotating a half-wave plate. NDF, neutral density filter; HNF, holographic notch filter. (b) A typical low-frequency spectrum of 1-hexadecanethiol adsorbed onto a silver nanowire monolayer. The probe size was approximately 5 μm^2. The predominance of trans peaks indicates solidlike packing that extends into the hydrocarbon tails.

shown in Figure 2a. A green diode-pumped solid-state laser at 532 nm was used as the excitation source. To prevent sample degradation and overheating, a neutral density filter (NDF) was used to decrease the laser power at the sample to approximately 0.2 mW. The laser was directed through a polarizer and focused onto the sample through a 100× objective (NA = 0.95). Scattered light was collected through the same objective and directed to a spectrometer equipped with a CCD detector. The total collection time for each spectrum was approximately 30 s. Once Raman spectra were recorded, the nanowire assemblies were characterized by SEM. By noting the coordinates of the underlying TEM grid, SEM images of the nanowires were correlated with their corresponding Raman spectra.

A typical low-frequency SERS spectrum for a thiol-coated nanowire film is shown in Figure 2b. The $C-S_{trans}$ (700 cm^{-1}) and $C-C_{trans}$ bands (1000−1200 cm^{-1}) are indicative of a well-ordered thiol monolayer at the silver surface; the predominantly trans C−H bands at 890, 1290, and 1430 cm^{-1} suggest this ordering extends into the hydrocarbon tails of the monolayer.[19] Intensities for these low-frequency bands were collected for different polarizations of incident light. The spectra in Figure 3 were recorded by rotating a half-wave plate in the laser path by increments of 10°. As the angle θ between the polarized electric field and the long axes of the nanowires (Figure 3a, inset) approaches 90°, the SERS intensity reaches a maximum. Minimum intensities were obtained at $\theta = 0°$ and $\theta = 180°$.

To outline this periodicity, SERS intensities were plotted as a function of θ for each individual Raman band (Figure 3b). Interestingly, all Raman bands experience the same intensity fluctuations with respect to θ, with maxima at 90 and 270°. This angular dependence is unexpected for surface enhancement from a single nanowire: the literature suggests maximum SERS intensities are obtained when the incident field is parallel to the wire.[25] This occurs with excitation of the long-axis plasmon resonance. In the "lightning rod effect", intense local electromagnetic fields emanate from points of high curvature, such as the tip of a rod or wire.[26,27] Our data, however, indicate that the local field responsible for the enhanced Raman signal is dipolar and oriented perpendicular to the long axes of the wires but not localized at the nanowire ends.

Rather, this polarization dependence suggests that nanowire junctions serve as local Raman hot spots. At an excitation wavelength of 532 nm, surface enhancement arising from pairwise EM interactions dominates the collected SERS signal. If the interwire distance is sufficiently small (<10 nm), incident radiation can excite a new plasmon mode trapped between adjacent, parallel wires. This plasmon band was previously observed in UV−vis absorption spectra as a broad peak centered at 500 nm, in contrast with the spectrum for isolated silver nanowires, which exhibited a single peak at 380 nm.[19] Because the plasmon band for isolated wires is far from our excitation wavelength, the SERS signal most likely ensued from preferential excitation of this coupled plasmon mode. Considering the large aspect ratio of the nanowires, it is also unlikely that the longitudinal plasmon mode for a single wire could be excited at this wavelength. It should also be noted that Raman bands (for both hexadecanethiol and rhodamine 6G) were not detected

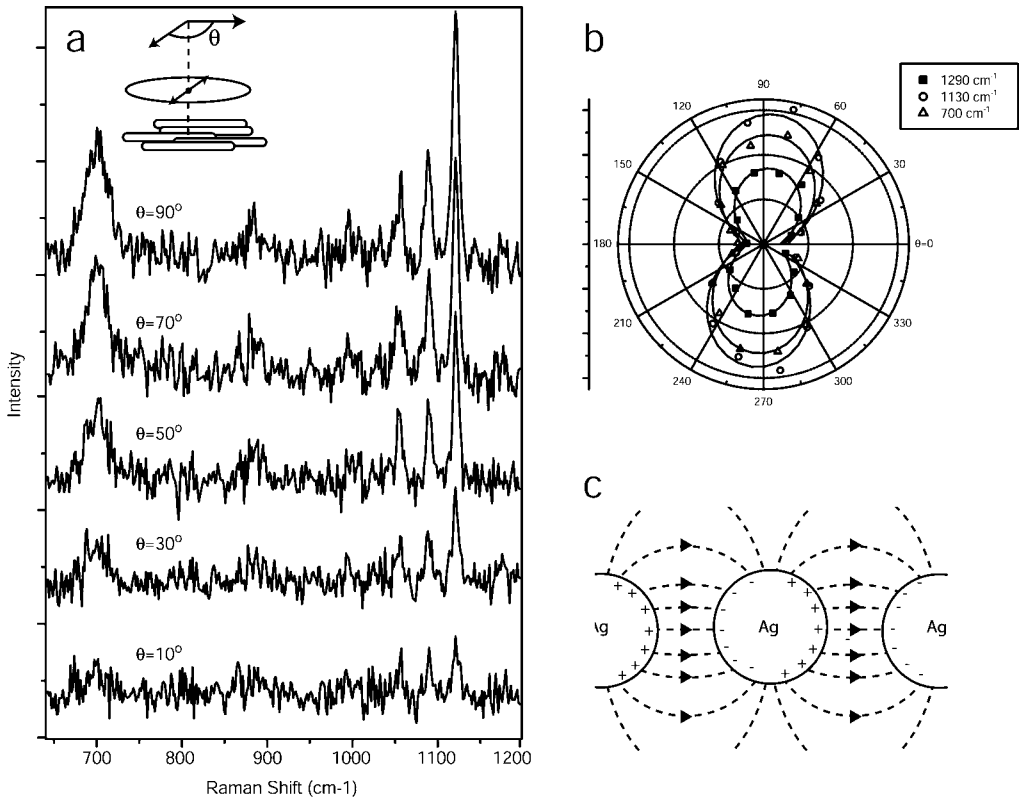

Figure 3. (a) SERS spectra of adsorbed 1-hexadecanethiol on a nanowire monolayer taken at different polarization directions of incident light. The angle θ is taken as the difference between the polarization direction and the long nanowire axis, as shown in the inset. The maximum SERS signal is collected at $\theta = 90°$. (b) Polar plot of SERS intensities for various low-frequency Raman bands with respect to polarization angle. The dark lines represent the best fit to a periodic cosine function. (c) Schematic illustration of the electromagnetic field generated between two adjacent nanowires upon incident irradiation, shown in a cross-sectional view. The surfaces on opposing sides of the junction have opposite polarization charges, leading to the highly dipolar nature of this geometry.

for isolated nanowires using the same experimental configuration. The isolated nanowires were prepared by drop-casting a sufficiently diluted nanowire solution onto the substrate.

Our experimental observations correlate well with the predictions by Garcia-Vidal and Pendry, who modeled EM coupling between aligned silver half-cylinders.[6] According to their calculations, incident radiation excites a plasmon trapped in the interstitials between cylinders, which can lead to SERS enhancements as large as 10^7. In particular, this occurs for cylinder dimensions smaller than the excitation wavelength. Their model also indicates that polarization charges on either side of the gap oppose each other to produce a highly dipolar field, which is consistent with the observed angular dependence of our nanowire system (see Figure 3).

For polarized incident light, the observed SERS intensities are expected to vary as $\cos^4 \theta$ according to eq 1. (Typically, the scattering frequency and frequency of incident radiation are approximated as being equal.) Instead, a $\cos^2 \theta$ dependence was observed. The solid lines in Figure 3b correspond to best fits using a $\cos^2 \theta$ function corrected for damping. This discrepancy was also reported for both gold stripes[28] and silver nanoparticle aggregates.[29] Brolo et al. attributed this inconsistency to two main causes: (1) the invalid approximation that $E(\omega) = E(\omega_s)$ and (2) the isotropic nature of the adsorbed molecule. The latter conjecture might not be applicable to our nanowire system: the long-chain thiol molecules assume a coherent, well-defined orientation relative to the silver surface. However, a third possibility is the excitation of higher-order surface plasmon modes, which may result from imperfect nanowire alignment or multiwire coupling.

To investigate long-range EM coupling across the nanowire film, we analyzed the polarization of the collected Raman signal as a function of nanowire alignment. Nanowire alignment was characterized by the order parameter, *S*, according to

$$S = \frac{1}{2}\langle 3 \cos^2 \phi - 1 \rangle \qquad (2)$$

where ϕ is the angle between a specific nanowire and the average director for the assembly. These ϕ values were obtained from SEM images of the nanowires, taken after completing all Raman measurements to avoid hydrocarbon degradation from the electron beam. Polarization studies were performed on 30 samples with varying degrees of order, exemplified by Figure 1. The angular-dependent SERS intensities for low-frequency Raman bands were fit to $\cos^2 \theta$ functions, as discussed earlier. Figure 4 shows the goodness-of-fit values, R^2, plotted against *S*. We expected well-aligned films to produce greater dipolar scattering given the higher density of parallel wire junctions, and as we can see in this figure, the degree of polarization increases with better sample order. The heterodasticity in the data, prevalent for data points of low order, is attributed to the assignment of *S*; because it is an averaged value, the order parameter is probably less reliable in characterizing samples that possess poor long-range alignment but a high degree of local order. Such monolayers have a high number of nanowire junctions despite low *S* values.

We used single-crystalline silver nanowires with exceedingly uniform shape, size, and surfaces to give SERS signals that are highly dipolar and exhibit large enhancement factors. The observed dependence on polarization direction confirms prior theoretical predictions that large EM fields are localized in the interstitials between adjacent nanowires. We show that these modes are largely dipolar in nature and rely on short-range EM

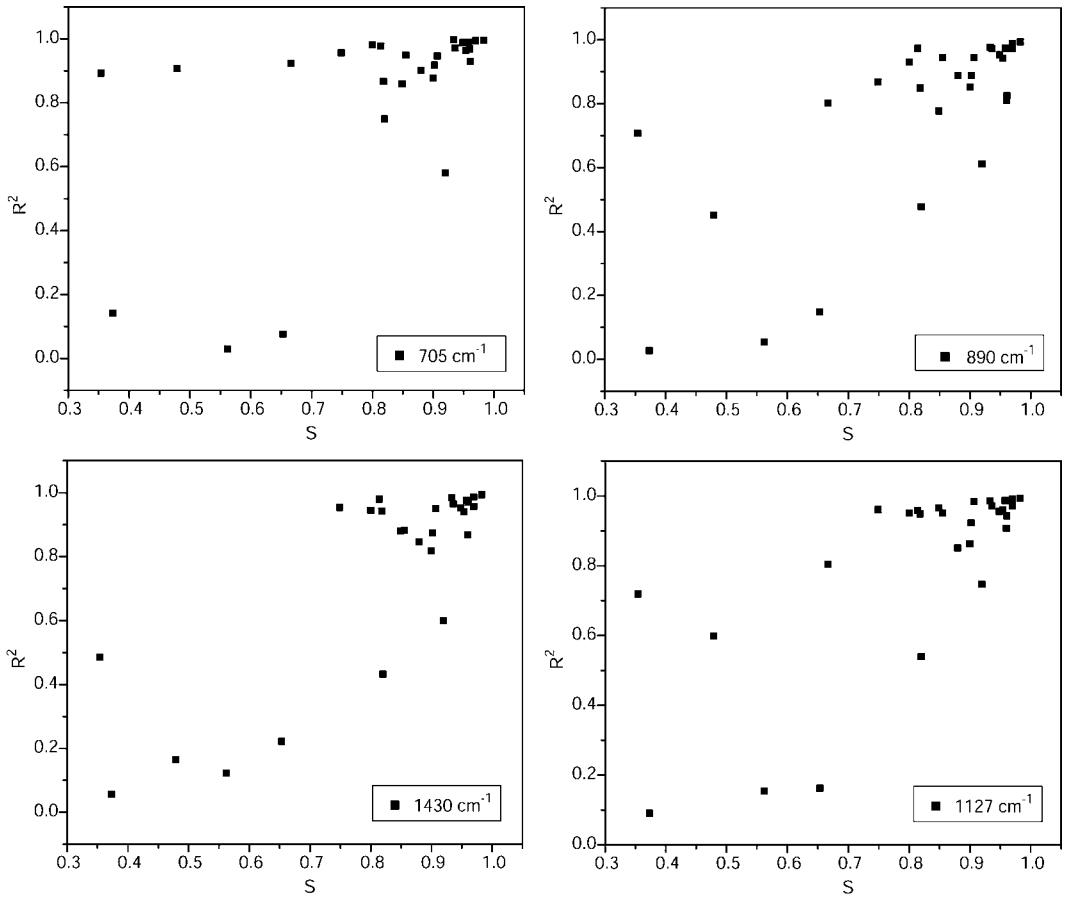

Figure 4. Plot showing the change in SERS signal polarity with respect to nanowire film alignment. The goodness-of-fit variable, R^2, indicates the degree of bipolarity for a specific sample. Each plotted point represents one nanowire film for which polarized SERS experiments were performed.

coupling between nanowires. With this in mind, it should be possible to engineer specific adsorption sites in nanostructure junctions to create electromagnetic hot spots with predictable EM responses.

Acknowledgment. This work was supported in part by the Department of Energy and the National Science Foundation. A.R.T. thanks the National Science Foundation for a graduate fellowship. Work at the Lawrence Berkeley National Laboratory was supported by the Office of Science, Basic Energy Sciences, Division of Materials Science, of the U. S. Department of Energy. We thank the National Center for Electron Microscopy for the use of their facilities.

References and Notes

(1) Nie, S.; Emory, S. R. *Science (Washington, D.C.)* **1997**, *275* (5303), 1102−1106.
(2) Kneipp, K.; Wang, Y.; Kneipp, H.; Perelman, L. T.; Itzkan, I.; Dasari, R. R.; Feld, M. S. *Phys. Rev. Lett.* **1997**, *78* (9), 1667−1670.
(3) Kneipp, K.; Kneipp, H.; Itzkan, I.; Dasari, R. R.; Feld, M. S. **1999**, *99* (10), 2957−2975.
(4) Michaels, A. M.; Jiang, J.; Brus, L. *J. Phys. Chem. B* **2000**, *104* (50), 11965−11971.
(5) Kottmann, J. P.; Martin, O. J. F. *Opt. Express* **2001**, *8* (12), 655−663.
(6) Garcia-Vidal, F. J.; Pendry, J. B. *Phys. Rev. Lett.* **1996**, *77* (6), 1163−1166.
(7) Albano, E. V.; Daiser, S.; Ertl, G.; Miranda, R.; Wandelt, K.; Garcia, N. *Phys. Rev. Lett.* **1983**, *51* (25), 2314−2317.
(8) Wood, T. H.; Zwemer, D. A.; Shank, C. V.; Rowe, J. E. *Chem. Phys. Lett.* **1981**, *82* (1), 5−8.
(9) Tuschel, D. D.; Pemberton, J. E.; Cook, J. E. *Langmuir* **1986**, *2* (4), 380−388.
(10) Yang, X. M.; Ajito, K.; Tryk, D. A.; Hashimoto, K.; Fujishima, A. *J. Phys. Chem.* **1996**, *100* (18), 7293−7297.
(11) Pockrand, I. *Chem. Phys. Lett.* **1982**, *85* (1), 37−42.
(12) Albano, E. V.; Daiser, S.; Miranda, R.; Wandelt, K. *Surf. Sci.* **1985**, *150* (2), 367−385.
(13) Goudonnet, J. P.; Bijeon, J. L.; Warmack, R. J.; Ferrell, T. L. *Phys. Rev. B: Condens. Matter Mater. Phys.* **1991**, *43* (6), 4605−4612.
(14) Jensen, T. R.; Malinsky, M. D.; Haynes, C. L.; van Duyne, R. P. *J. Phys. Chem. B* **2000**, *104* (45), 10549−10556.
(15) Haynes, C. L.; Van Duyne, R. P. *Nano Lett.* **2003**, *3* (7), 939−943.
(16) Shafer-Peltier Karen, E.; Haynes Christy, L.; Glucksberg Matthew, R.; Van Duyne Richard, P. *J. Am. Chem. Soc.* **2003**, *125* (2), 588−593.
(17) Zheng, J.; Zhou, Y.; Li, X.; Ji, Y.; Lu, T.; Gu, R. *Langmuir* **2003**, *19* (3), 632−636.
(18) Xu, H.; Bjerneld, E. J.; Käll, M.; Börjesson, L. *Phys. Rev. Lett.* **1999**, *83* (21), 4357−4360.
(19) Tao, A.; Kim, F.; Hess, C.; Goldberger, J.; He, R.; Sun, Y.; Xia, Y.; Yang, P. *Nano Lett.* **2003**, *3* (9), 1229−1233.
(20) Jeong, D. H.; Zhang, Y. X.; Moskovits, M. *J. Phys. Chem. B* **2004**, *108* (34), 12724−12728.
(21) Haynes, C. L.; McFarland, A. D.; Zhao, L.; Van Duyne, R. P.; Schatz, G. C.; Gunnarsson, L.; Prikulis, J.; Kasemo, B.; Kaell, M. *J. Phys. Chem. B* **2003**, *107* (30), 7337−7342.
(22) Freeman, R. G.; Grabar, K. C.; Allison, K. J.; Bright, R. M.; Davis, J. A.; Guthrie, A. P.; Hommer, M. B.; Jackson, M. A.; Smith, P. C.; et al. *Science (Washington, D.C.)* **1995**, *267* (5204), 1629−1631.
(23) Sun, Y.; Mayers, B.; Herricks, T.; Xia, Y. *Nano Lett.* **2003**, *3* (7), 955−960.
(24) Koglin, E.; Schwuger, M. J. *Faraday Discuss.* **1992**, *94*, 213−220.
(25) Sonnichsen, C.; Franzl, T.; Wilk, T.; von Plessen, G.; Feldmann, J.; Wilson, O.; Mulvaney, P. *Phys. Rev. Lett.* **2002**, *88* (7), 077402/1−077402/4.
(26) Hao, E.; Schatz, G. C. *J. Chem. Phys.* **2004**, *120* (1), 357−366.
(27) Jiang, J.; Bosnick, K.; Maillard, M.; Brus, L. *J. Phys. Chem. B* **2003**, *107* (37), 9964−9972.
(28) Brolo, A. G.; Arctander, E.; Addison, C. J. *J. Phys. Chem. B* **2005**, *109*, 401−405.
(29) Itoh, T.; Hashimoto, K.; Ozaki, Y. *Appl. Phys. Lett.* **2003**, *83* (11), 2274−2276.